

Numerical analysis of the behaviour of repaired surface cracks with bonded composite patch

Mohamed Merzoug^a, Abdelkader Boulenouar^{*} and Mohamed Benguediab^b

Laboratory of Materials and Reactive Systems - LMSR. University of Sidi Bel Abbes. BP. 89, City Larbi Ben Mhidi. Sidi Bel Abbes, Algeria

(Received May 26, 2016, Revised June 01, 2017, Accepted July 16, 2017)

Abstract. In this paper, the analysis of the behavior of surface cracks in finite-thickness plates repaired with a Boron/Epoxy composite patch is investigated using three-dimensional finite element methods. The stress intensity factor at the crack-front was used as the fracture criteria. Using the Ansys Parametric Design Language (APDL), the stress intensities at the internal and external positions of repaired surface crack were compared. The effects of the mechanical and geometrical properties of the adhesive layer and the composite patch on the variation of the stress intensity factor at the crack-front were examined.

Keywords: patch; stress intensity factor; surface cracks; bonded composite repairs

1. Introduction

Due to various benefits of composite materials such as light weight, high strength and their excellent formability, the externally bonded composite patches have been proved to be a preferable method of repairing flaws and cracks in various engineering structures. This repairing method initially was investigated in Australia in early 1970s (Baker 1980, 1984, Baker *et al.* 1984) and later in USA in 1980s. Later on, considerable studies have been performed to develop this technology by various experimental (Srilakshmi and Ramji 2012) and numerical methods. Among them Jones and Callinan (1979), Bachir *et al.* (2002), Chung and Yang (2002), Kumar and Singh (1997), and Ayatollahi and Hashemi (2007) have used the finite element method to investigate the effect of composite patching on the stress intensity factor of crack, as an important measure for analyzing the performance of composite reinforcement technique.

The determination of the stress intensity factors at the crack tip is one of the possible means to analyze the performance of the bonded composite repairs. It is known that the finite element method gives, with a great accuracy, the stress intensity factors at the crack tip. Ramji *et al.* (2013) investigated the 3D finite element analysis to get an optimum composite patch shape applied on an inclined center cracked panel, repaired by symmetrical patch. Bezzerouki *et al.* (2011) analysed the behavior of cracked pipeline repaired with bonded composite wrap subjected to traction effect is performed using 3D finite element methods. Boulenouar *et al.* (2013a) analyzed the SIFs

variation for repaired semi-circular surface cracks in finite-thickness plates with bonded composite patch subjected to traction loading. Mhamdia *et al.* (2011) studied the effects of the thermal residual stresses on the variation of the SIF for repaired aluminum crack with boron/epoxy and graphite epoxy patches using the 3D finite element method. Hosseini-Toudeshky *et al.* (2012) investigated the 3D finite element analyses to study the effects of various characteristics of both repair and stiffeners' on fatigue crack growth of stiffened panels and repaired with composite patches. Jian-Bin *et al.* (2015) evaluated the fatigue life and fatigue crack growth rates in aluminum panels repaired with two sided bonded patches. The SIF values of the patched plates were obtained by using 3D finite element method. Hosseini-Toudeshky and Mohammadi (2009) studied the fatigue crack growth of repaired thick aluminum panels containing a central inclined crack repaired on one side with glass/epoxy composite patches. The finite element analyses were performed assuming uniform crack growth along the panel's thickness to simplify the analyses. Bachir Bouiadja *et al.* (2012) analysed the effect of the adhesive disband for inclined cracks repaired with boron/epoxy patch. It was concluded that the both mode I and mode II stress intensity factors are negatively affected by the presence of the adhesive disbond. Gu *et al.* (2011) developed the 3D finite element models to quantify the performance of pre-cracked Al 7075-T6 Single Edge Notch Tension (SENT) specimen repaired with various bonded composite patches. Srilakshmi *et al.* (2015) investigated the fatigue life of unrepaired and repaired Al-2014-T6 panels with an inclined center crack. The fatigue life obtained from experiments is compared against the FEA predictions quantitatively. Ouinas *et al.* (2012) studied the crack growth behaviour of an aluminium plate cracked at the tip and repaired with a bonded Boron/Epoxy composite patch in the case of full-width disbond. Albedah *et al.* (2013) studied the stress intensity factor for crack emanating from central holes and repaired with bonded composite patch in aircraft structures. Maligno

*Corresponding author, Ph.D.,

E-mail: aek_boulenouar@yahoo.fr

^a Ph.D., E-mail: m_merzoug01@yahoo.fr

^b PEhD., E-mail: benguediab_m@yahoo.fr

et al. (2013) investigated the software Zencrack in combination with the 3D FE code ABAQUS to simulate the fatigue crack growth behaviour in an aluminium panel repaired with a bonded composite patch.

The aim of this paper is to investigate the effects of composite reinforcement on the behaviour of surface cracks in finite-thickness plates using the three-dimensional finite element method. Various authors showed that in practice the parameters influencing the performances of the bonded composite repairs are the patch and the adhesive properties. For that, the effects of single patch thickness and mechanical and geometrical properties of the adhesive on the variations of the stress intensity factor along the crack front are highlighted.

2. Geometrical model

The basic geometry of a semi-circular crack in a plate under mode-I loading was considered with the following dimensions: height $2H = 60$ mm, width $2W = 60$ mm and thickness $t = 15$ mm (Fig. 1).

The surface crack of ray (a) is repaired with Boron-Epoxy composite patch bonded with FM73 adhesive having thickness $e_{adh} = 0.2$ mm. The dimensions of the single patch are: $H_{patch} = 25$ m, $W_{patch} = 12$ mm and $e_{patch} = 2$ m, where H_{patch} , W_{patch} and e_{patch} represents the height, width, and thickness of composite patch,

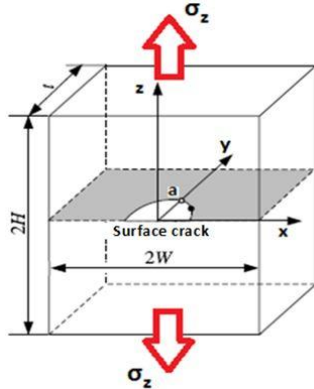


Fig. 1 Surface semi-circular crack in a finite plate under mode-I loading

Table 1 Materials properties (Plate, Patch and Adhesive)

	Al-Alloy 024-T3	Boron/Epoxy	Adhesive FM73
E_1 (GPa)	72	200	2.55
E_2 (GPa)	-	19.6	-
E_3 (GPa)	-	19.6	-
G_{12} (GPa)	-	7.2	-
G_{13} (GPa)	-	5.5	-
G_{23} (GPa)	-	5.5	-
ν_{12}	0.33	0.3	0.32
ν_{13}	-	0.3	-
ν_{23}	-	0.28	-

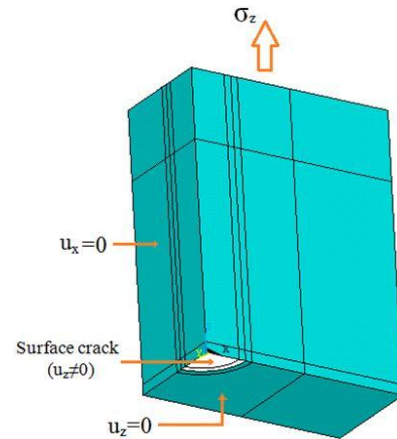


Fig. 2 Boundary conditions and applied load

respectively. The elastic aluminum plate is submitted under a uniform tensile load $\sigma = 60$ Mpa at the both ends.

3. Finite element model

The analysis involves a three-dimensional finite element method by using a commercially available finite element code Ansys.11. The finite element model consists of three subsections to model the cracked plate, the adhesive, and the composite patch.

The problem is symmetric in both the plate's width and height directions; only quarter of the plate is modeled including half of the top crack surface. In Fig. 2, the quarter plate model containing a semi-circular surface crack with symmetry boundary conditions is shown.

For meshing technique, two element types are used: MESH-200 and SOLID-186.

MESH-200; is a mesh-only element, does not contribute to the solution. We could have simply meshed the entire volume with SOLID-186 elements. However, the advantage to first meshing an area with MESH-200 element is that it provides greater control over element sizes.

SOLID-186; is a 3-D, 20-Node structural solid element. The element is defined by 20 nodes having three degrees of freedom per node: translations in the nodal x , y , and z directions. In this study prism option is used around the crack front as singular elements.

To create a mesh surrounding the crack front, the area mesh is created with 2D singular elements proposed by Barsoum, using mesh-200 element. Later, this area is swept to generate volume with surface crack, using 20-noded solid-186 element. Fig. 3(a) shows the overall mesh of the plate and mesh refinement near the crack region.

Other structured area mesh is created and later all the areas are dragging in width direction to generate volume as shown in Fig. 3(b).

The patch and adhesive are modeled with 20-noded solid elements as per the dimensions shown in Fig. 3(c). In the thickness direction, the adhesive and the patch are meshed with three elements.

The position of a point on the crack front is defined by the angle φ (Fig. 4). φ takes the value of 90° at the deepest point (point N) and 0° at the surface point (point M).

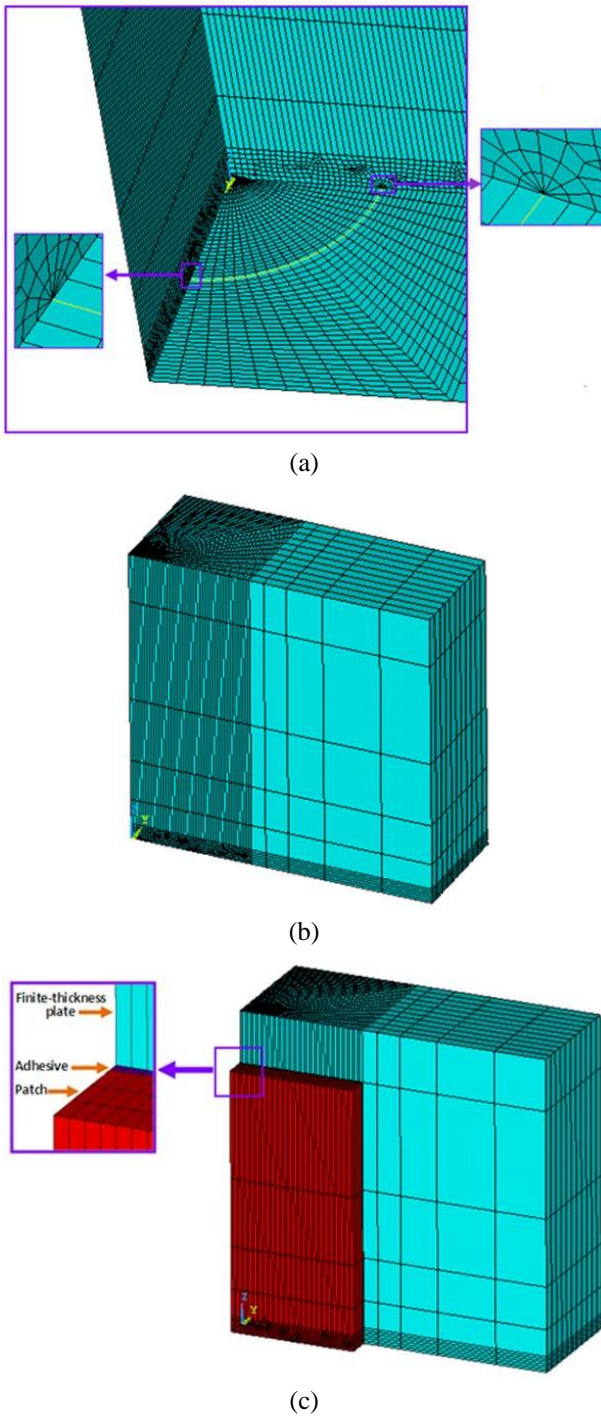


Fig. 3 (a) Meshes near the crack front; (b) FE model of the plate without patch; (c) Typical mesh model for bonded patch repairs

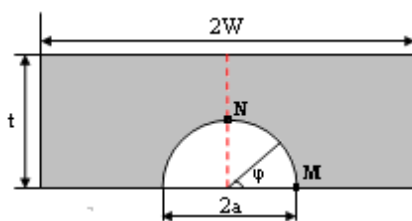


Fig. 4 Schematic of a surface semi-circular crack in a finite plate

4. SIFs and J-integral formulation

In linear elastic material response, the stress intensity factor in opening mode K_I can be computed from the J-integral by

$$K_I = \sqrt{JE'} \quad (1)$$

Where $E' = E$ for plane stress condition and $E' = E/(1 - \nu^2)$ for plane strain condition, E is the modulus of elasticity, and ν is the Poisson's ratio.

The present study employs the domain-integral approach, as originally developed by Shih *et al.* (1986) to compute the energy release rate along the curved front of the surface crack in three dimensions. The local value of the strain energy release rate, denoted $J(z)$, at each point s on a planar, non-growing crack front under general dynamic loading is given by

$$J(z) = \lim_{\Gamma \rightarrow 0} \int_{\Gamma} \left[(W_s + T)n_1 - P_{ij} \frac{\partial u_i}{\partial X_i} n_i \right] d\Gamma \quad (2)$$

where W_s and T are respectively the stress-work density and the kinetic energy density per unit volume at initial configuration; Γ is a vanishingly small contour which lies in the principal normal plane at crack front, and n_1, n_2, n_3 are the unit vectors referred to X_1, X_2, X_3 local orthogonal coordinate system. P_{ij} denotes the non-symmetric 1st Piola-Kirchoff stress tensor which is work conjugate to the displacement gradient, $\partial u_i / \partial X_i$, expressed on the initial configuration; thus the stress-work rate per unit volume at initial configuration is simply $P_{ij} \partial u_i / \partial X_i$. All field quantities are expressed in the above mentioned local orthogonal coordinate system (X_1, X_2, X_3 shown in Figs. 5(a) and (b)) at location z on the crack front (Fig. 5(a)). For plane stress and plane strain conditions, with nonlinear elastic material response and small strain theory, $J(z)$ of Eq. (2) simplifies to the well known J-integral as explained by Rice (1968) that exhibits global path independence.

The direct evaluation of Eq. (2) is cumbersome in a finite element model due to the geometric difficulties encountered in defining a contour that passes through the integration points. Moreover, the limiting definition of the contour requires extensive mesh refinements near the crack tip to obtain meaningful results. In this work, numerical J-integral values have been evaluated by using the equivalent domain integral (EDI) technique (Nikishkov and

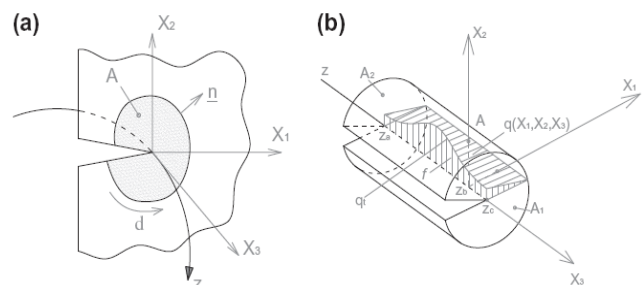


Fig. 5 Functions used in EDI

Atluri 1987), as well as it is implemented in the ANSYS code.

By using a weight function ($q_t(z)$ Fig. 5(b)), which may be interpreted as a virtual displacement field, the contour integral $J(z)$ of Eq. (2) is converted into an area integral for two dimensions and into a volume integral $J(z_a - z_c)$ for three dimensions (Murakami 1985 and Li *et al.* 1985). Body forces (other than inertial loading) are assumed to be zero. The resulting expressions are

$$\begin{aligned} \underline{J}_{z_a-z_c} &= \left[\int_{z_a}^{z_c} J(z) q_t(z) dz \right] \\ &= \int_{V_0} \left[P_{ji} \frac{\partial u_i}{\partial X_k} \frac{\partial q_k}{\partial X_j} - W_s \frac{\partial q_k}{\partial X_k} \right] dV_0 = \underline{J} \end{aligned} \quad (3)$$

Where q_k denotes a component of the vector weight function in the k coordinate direction, V_0 represents the volume of the domain surrounding the crack tip in the (undeformed) initial configuration, and z denotes positions along the crack front segment. It should be point out that the vector function q is directed parallel to the direction of crack extension. When all field quantities of the finite element solution are transformed to the local crack front coordinate system at point z and Mode-I extension is considered; only the q_1 term of the weight function is non zero. In subsequent discussions, this transformation to the (local) crack front coordinate system is assumed to hold; therefore q_k means the q_1 term. $J(z)$ is the local energy release rate that corresponds to the perturbation of $q_t(z)$ at point z . Fig. 5 shows a typical domain volume defined for an internal segment along a three dimensional surface crack.

The value of q_1 at each point in the volume V_0 is readily interpreted as the virtual displacement of a material point due to the virtual extension of the crack front $q_t(z)$. An approximate value of $J(z_b)$ is obtained by applying the mean value theorem over the interval z_a, z_c . The point wise value of the J-integral at z_b is given by (Fig. 5(b))

$$J(z = z_b) \approx \frac{\left[\int_{z_a}^{z_c} J(z) q_t(z) dz \right]}{\left[\int_{z_a}^{z_c} q_t(z) dz \right]} = \frac{J}{f} \quad (4)$$

In Eq. (4), " z_a " and " z_c " are the abscissas along crack front of initial and final nodes of the considered portion of crack front, $J(z)$ is the J-Integral value and $q_t(z)$ is the resultant value of q -function at position " z " between " z_a " and " z_c ". The q -function is defined within an element domain by using its own shape function. As a matter of fact, in Eq. (4) the numerator, J , is the energy released as a consequence of a virtual extension of the crack, while the denominator, f , is the increase of crack area following the same virtual increase. For common through crack test specimens the crack front is generally straight or only slightly curved. For such crack geometries, the average J for the entire crack front value is obtained by the application of a uniform $q_t(z)$ across the full crack front. With those assumptions numerical evaluation of the J requires only straightforward application of isoparametric

element techniques once the computed field quantities are transformed from the global X, Y, Z coordinate system to the X_1, X_2, X_3 local (crack front) system at point z on the front. In this simplified form, Eq. (3) becomes

$$\underline{J} = \int_{V_0} \left[P_{ij} \frac{\partial u_i}{\partial X_i} \frac{\partial q_1}{\partial X_j} - W_s \frac{\partial q_1}{\partial X_k} \right] dV_0 \quad (5)$$

It must be stressed that volume integrals are numerically evaluated by using the same Gauss technique adopted to generate the elemental stiffness matrix and that the formulation of the q -function is consistent with the isoparametric one used to represent the element behaviour.

In FE code ANSYS; the domain integration formulation applies the volume integration for 3D problems. This procedure requires the data of the nodes forming the crack front and a mesh concentric around the crack front to ensure a good evaluation of the SIF and the J-integral. This FE code has been used successfully in several numerical works (Boulenouar *et al.* 2016, Benamara *et al.* 2017a and b).

5. Analysis and results

5.1 Comparison between repaired and non-repaired semi-circular surface crack

Fig. 6 shows the variation of SIF K_I along the crack front in finite-thickness plate repaired and non-repaired, with $a = 6$ mm. Repaired specimen with bonded composite patch of the surface crack presents a remarkable reduction of the SIF along the crack front.

For a crack emerging at the surface, there are two particular points: the deepest point ($\varphi = 90^\circ$) and the point where the crack emerges indicated as the surface point ($\varphi = 0^\circ$). In general, the analysis of propagation at these two points is enough to judge the severity of the defect. For this reason, we restricted the analysis of our results to these two points.

Fig. 6 represents the SIF variation as a function of the parameter a , at the deepest and the surface points of the

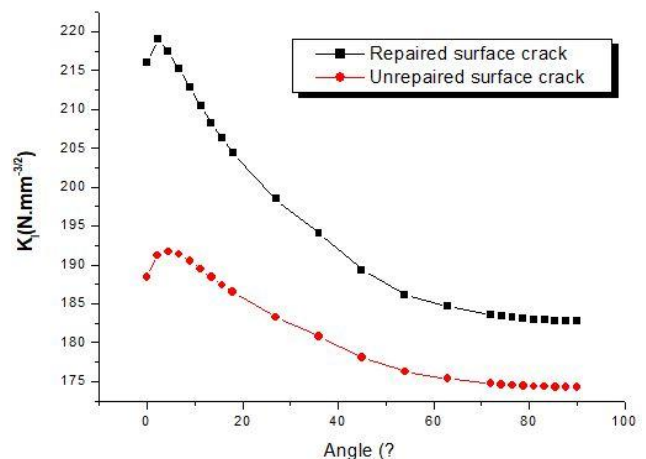


Fig. 6 Variation of the SIF along the semi-circular crack front

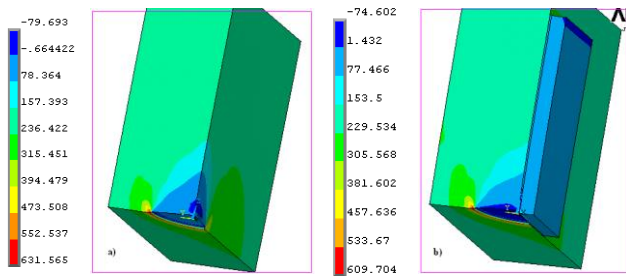


Fig. 7 Contour of stresses σ_z around the crack front ($a = 6 \text{ mm}$)

crack front. The repair with bonded composite patch at the surface point ($\varphi = 0^\circ$) presents a considerable reduction of the SIF than noticed at the deepest point ($\varphi = 90^\circ$).

This behavior is due to the direct contact of the external face of the crack with the adhesive layer and the patch. The transfer of load between the composite patch and the semi-circular surface crack through the adhesive layer is maximum for $\varphi = 0^\circ$.

The resolution by finite elements enables us to give in Fig. 7, the contour of stresses σ_z around the crack front in a repaired and non-repaired plate. The beneficial effect of the patch is definitely visible because these stresses strongly decrease; it is owing to the fact that the patch absorbs the efforts load transferred by the plate through the adhesive.

5.2 Influence of the adhesive thickness (e_{adh})

The adhesive thickness is an essential parameter for the mechanical resistance of adhesion and the transfer load. The study of its effect on the criteria of reinforced crack propagation is of a great utility. Fig. 8 presents the SIF variation all along semi-circular crack front repaired with composite patch, for various values of adhesive thickness (e_{adh}). This figure shows that a less smaller thickness of adhesive led to a reduction of the SIF. The stabilization of the crack requires the use of adhesive thin. To ensure at the same time a good adherence and a good an effective stress transfer, the adhesive thickness requires an optimization

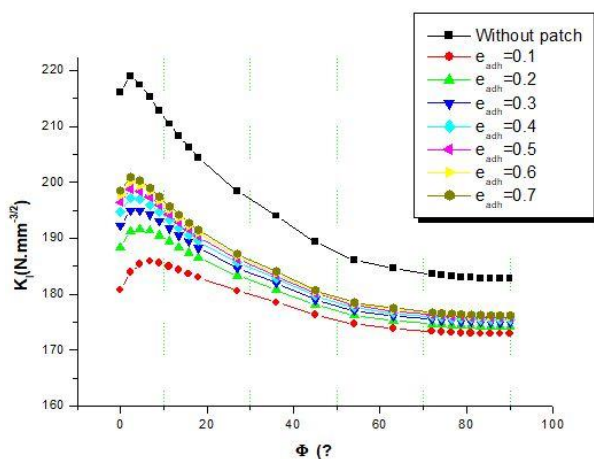


Fig. 8 Effect of the adhesive thickness on the SIF along the crack front

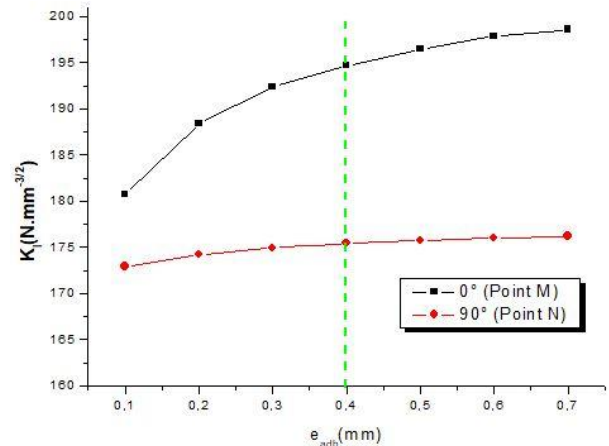


Fig. 9 Variation of the SIF according to the adhesive thickness, for $\varphi = 0^\circ$ and 90°

because a thin adhesive ensures a good transfer and a weak energy of adhesion plates/patch. This effect was highlighted by Turaga and Ripudaman (1999), Achour *et al.* (2003) and Bezzerouki *et al.* (2011).

Fig. 9 illustrates the evolution of the SIF according to the adhesive thickness at the points M and N. We notice that the effect the adhesive thickness is negligible at the interns position ($\varphi = 90^\circ$). While, at the external position ($\varphi = 0^\circ$), the increase adhesive thickness increases the SIF for an interval of 0.1 to 0.4 mm. Beyond this value, the SIF varies very little with the increase of the adhesive thickness. Boulenouar *et al.* (2013b) and Benamara *et al.* (2015) showed that the increase in the adhesive thickness leads to the increase of the SIF, especially for external positions of crack-front repaired semi-circular surface cracks. Bezzerouki *et al.* (2011) observed that the Young modulus of the adhesive is inversely proportional to the SIF. A high Young modulus allows a good transfer of the stresses and generates the greater reduction in SIF.

5.3 Effect of the adhesive Young's modulus (E_{adh})

The high stiffness (high Young's modulus) is an advantageous character for an adhesive of repair, which facilitates the stress load transfer through the adhesive towards the patch of repair and to the patch. Figure 10 presents the variation of the SIF along the semi-circular crack front, for various adhesive Young's modulus (E_{adh}). Indeed, the reductions in the SIF are directly proportional to the increase in the adhesive Young's modulus.

In reality, an increase in the adhesive Young's modulus reduces the mechanical attachment bonding strength, which leads results in weak adhesion. Therefore, the choice of adhesive for the repair of this cracks type must be optimized to allow firstly, the stress transfer to the patch, and to ensure a better adherence plates/patch.

Fig. 11 shows the variation of K_I according to the adhesive Young's modulus (E_{adh}) for the two points on the crack front. The results obtained show that the adhesive Young's modulus effect is negligible in the depth (Point M). While, the increase of the Young's modulus decreases appreciably, the SIF on the surface (Point N). This behavior

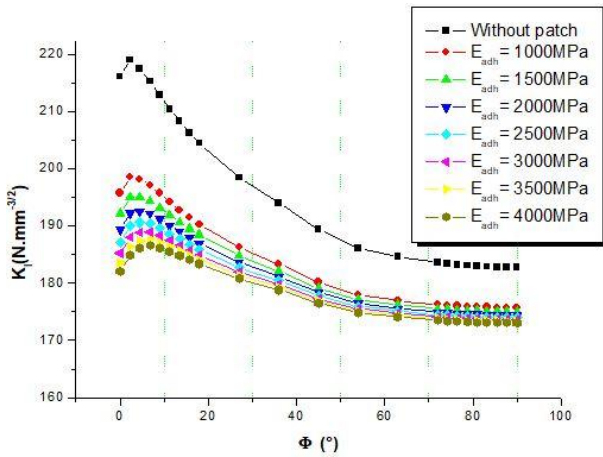


Fig. 10 Effect of the adhesive Young's modulus on the variation of the SIF along the crack front

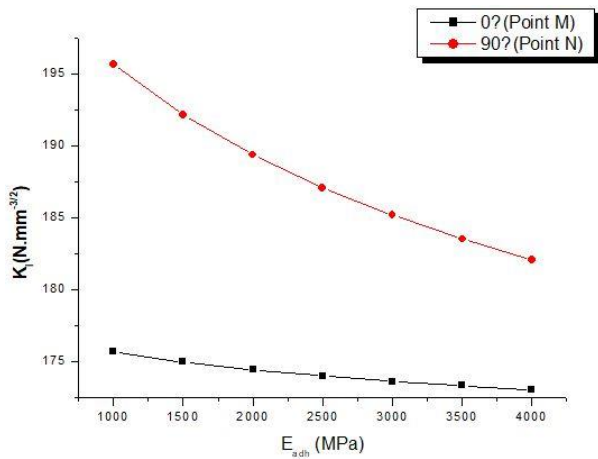


Fig. 11 Variation of the SIF according to the adhesive Young's modulus, for $\phi = 0^\circ$ and 90°

is due to the direct contact of the external face of the crack with the adhesive layer and the patch. As example, the ratio reduction of the SIF between 1000 MPa and 4000 MPa is about 24%.

5.4 Influence of the patch thickness (e_{patch})

Fig. 12 shows the variation of the SIF along the crack front, according to the patch thickness (e_{patch}). Our results show that the increase in patch thickness reduces the SIF over all the points of the crack front in a way proportional. This behavior makes it possible to conclude that a thicker patch ensures a good stability of the crack by an effective transfer of the stress field around the crack. This confirms that the choice of the thick patch improves their performances. For a better distribution of this field it is preferable to use a patch containing several layers.

Several authors showed the importance of the effect of the patch thickness on the repair performance in damaged structures. Belhouari *et al.* (2004) showed that the SIF decreases asymptotically according to the thickness of the patch for double and single bonded repairs in symmetric composite structures. Ramji and Srilakshmi (2009)

examined the effect the patch thickness single- and double-sided patch on center-cracked aluminum panel. It is found that double-sided repair is more efficient than single-sided repair. Bezzerouki *et al.* (2008) showed that the increase of the patch thickness decreases the SIF, which is benefice for the double adhesive technique. Kaddouri *et al.* (2008) have confirmed that the choice of thicker patches improves the repair performances in aircraft structure. Boulouar *et al.* (2013a) studied the SIFs variation for repaired semi-circular surface cracks; the increase of the patch thickness reduces the stress intensity factor at the crack tip in a proportional way. Bezzerouki *et al.* (2011) analyzed the variation in the SIF according to the patch thickness for the internal and external positions of cracks in pipeline repaired with bonded composite wrap. The increased thickness of the patch decreases the SIF for two positions of the crack. A thick patch allows good transfert of the stresses loads. Ouinass *et al.* (2007a, b) showed that the thicker patch allows a good absorption of the stress field emitted by the crack.

Fig. 13 illustrates the variation of the SIF according to the patch thickness, at the deepest and surface points,

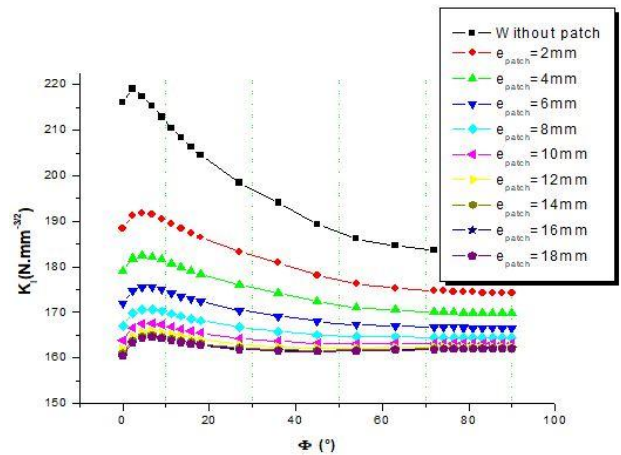


Fig. 12 Effect of the patch thickness on the SIF along the crack front

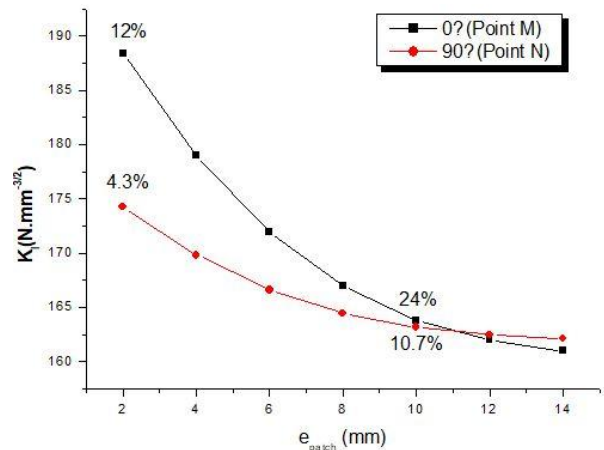


Fig. 13 Variation of the SIF according to the patch thickness, for $\phi = 0^\circ$ and 90° respectively. For these two points, the increase in patch

thickness leads to the reduction in the SIF. For patch thicknesses vary between 2 and 10 mm, the reduction of K_I amounts to 24% and 10.7%, for a crack at position M and N, respectively. Beyond this value of the patch thicknesses, the reduction in SIF with the increase patch thickness is marked very little. This result makes it possible to confirm that the choice of a thick patch which increases the performance of repair.

6. Conclusions

Using a three-dimensional finite element analysis, a study was carried out to characterize the effects of composite patching on fracture behavior of a surface cracks in finite-thickness plates, under mode-I loading conditions. The results obtained in this study allow us to deduce the following conclusions:

- The mode-I stress intensity factor along the crack front is reduced by the presence of the patch.
- The choice of the adhesive properties for repairing semi-circular surface crack, with the bonded composite patch, must be optimised.
- Low adhesive thicknesses ensure a good transfer of stresses. However, they increase the risk of the adhesive failure.
- For patch thicknesses vary between 2 and 10 mm, The reduction of K_I amounts to 24% and 10, 7%, at the external and internal positions of repaired surface crack, respectively. Beyond this value of the patch thicknesses, the reduction in SIF with the increase patch thickness is marked very little.
- The increase of the patch thickness reduces the stress intensity factor along the crack front.

References

- Achour, T., Bachir Bouiadjra, B. and Serier, B. (2003), "Numerical analysis of the performances of the bonded composite patch for reducing stress concentration and repairing cracks at notch", *Comput. Mater. Sci.*, **28**(1), 41-48.
- Albedah, A., Benyahia, F., Dinar, H. and Bachir Bouiadjra, B. (2013), "Analytical formulation of the stress intensity factor for crack emanating from central holes and repaired with bonded composite patch in aircraft structures", *Compos.: Part B*, **45**(1), 852-857.
- Ayatollahi, M.R. and Hashemi, R. (2007), "Computation of stress intensity factors (K_I , K_{II}) and T-stress for cracks reinforced by composite patching", *Compos. Struct.*, **78**(4), 602-609.
- Bachir Bouiadjra, B., Belhouari, M. and Serier, B. (2002), "Computation of the stress intensity factors for patched cracks with bonded composite patch in mode I and mixed mode", *Compos. Struct.*, **56**(4), 401-406.
- Bachir Bouiadjra, B., Oudad, W., Albedah, A., Benyahia, F. and Belhouari, M. (2012), "Effects of the adhesive disband on the performances of bonded composite repairs in aircraft structures", *Mater. Des.*, **37**, 89-95.
- Baker, A.A. (1981), "Bonded composite repair for fatigue-cracked primary aircraft structure", *Compos. Struct.*, **47**(1), 431-443.
- Baker, A.A. (1984), "Repair of cracked or defective metallic aircraft components with advanced fibre composites – an overview of Australian work", *Compos. Struct.*, **2**(2), 153-181.
- Baker, A.A., Callinan, R.J., Davis, M.J., Jones, R. and Williams, J.G. (1984), "Repair of Mirage III aircraft using BFRP crack-patching technique", *Theor. Appl. Fracture Mech.*, **2**(1), 1-16.
- Belhouari, M., Bachir Bouiadjra, B., Megueni, A. and Kaddouri, K. (2004), "Comparison of double and single bonded repairs to symmetric composite structures: A numerical analysis", *Compos. Struct.*, **65**(1), 47-53.
- Benamara, N., Boulenouar, A. and Aminallah, M. (2015), "Numerical analysis of the behaviour of repaired surface cracks with bonded composite patch", *Proceedings of the Institution of Mechanical Engineers, Part G: Journal of Aerospace Engineering*, Boumerdès, Algeria, November.
- Benamara, N., Boulenouar, A., Aminallah, M. and Benseddiq, N. (2017a), "On the mixed-mode crack propagation in FGMs plates: Comparison of different criteria", *Struct. Eng. Mech., Int. J.*, **61**(3), 371-379.
- Benamara, N., Boulenouar, A. and Aminallah, M. (2017b), "Strain energy density prediction of mixed-mode crack propagation in functionally graded materials", *Period. Polytech. Mech. Eng.*, **61**(1), 60-67.
- Bezzerrouki, M., Bachir Bouiadjra, B. and Ouinas, D. (2008), "SIF for cracks repaired with single composite patch having two adhesive bands and double symmetric one in aircraft structures", *Comput. Mater. Sci.*, **44**(2), 542-546.
- Bezzerrouki, M., Albedah, A., Bachir Bouiadjra, B., Ouddad, W. and Benyahia, F. (2011), "Computation of the stress intensity factor for repaired cracks with bonded composite wrap in pipes under traction effect", *J. Thermoplast. Compos.*, **26**(6), 831-844.
- Boulenouar, A., Aminallah, M. and Benamara, N. (2013a), "Computation of the SIF for repaired semi-circular surface cracks in finite-thickness plates with bonded composite patch", *J. Mater. Process. Environ.*, **1**(2), 121-127.
- Boulenouar, A., Benseddiq, N. and Mazari, M. (2013b), "Strain energy density prediction of crack propagation for 2D linear elastic materials", *Theor. Appl. Fract. Mec.*, **67-68**, 29-37.
- Boulenouar, A., Benseddiq, N., Merzoug, M., Benamara, N. and Mazari, M. (2016), "A strain energy density theory for mixed mode crack propagation in rubber-like materials", *J. Theor. Appl. Mech.*, **54**(4), 1417-1431.
- Chung, K.H. and Yang, W.H. (2002), "Fracture mechanics analysis on the bonded repair of a skin/stiffener with an inclined central crack", *Compos. Struct.*, **55**(3), 269-276.
- Jian-Bin, H., Xu-Dong, L. and Zhi-Tao, M. (2015), "Fatigue behavior of thick center cracked aluminum plates repaired by two-sided composite patching", *Mater. Des.*, **88**, 331-335.
- Jones, R. and Callinan, R.J. (1979), "Finite element analysis of patched cracks", *J. Struct. Mech.*, **7**(2), 107-130.
- Hosseini-Toudeshky, H. and Mohammadi, B. (2009), "Mixed-mode numerical and experimental fatigue crack growth analyses of thick aluminium panels repaired with composite patches", *Compos. Struct.*, **91**(1), 1-8.
- Hosseini-Toudeshky, H., Ghaffari, M.A. and Mohammadi, B. (2012), "Finite element fatigue propagation of induced cracks by stiffeners in repaired panels with composite patches", *Compos. Struct.*, **94**(5), 1771-1780.
- Gu, L., Kasavajhala, A.R.M. and Zhao, S. (2011), "Finite element analysis of cracks in aging aircraft structures with bonded composite-patch repairs", *Compos.: Part B*, **42**(3), 505-510.
- Kaddouri, K., Ouinas, D. and Bachir Bouiadjra, B. (2008), "FE analysis of the behaviour of octagonal bonded composite repair in aircraft structures", *Comput. Mater. Sci.*, **43**(4), 1109-1111.
- Kumar, A.M. and Singh, R. (1997), "3D finite element modelling of a composite patch repair", *Proceedings of the 9th International Conference on Fracture*, Sydney, Australia, April, pp. 2159-2166.
- Li, F.Z., Shih, C.F. and Needleman, A.A. (1985), "A comparison of methods for calculating energy release rates", *Engng. Fract.*

- Mech.*, **21**(2), 405-421.
- Maligno, A.R., Soutis, C. and Silberschmidt, V.V. (2013), "An advanced numerical tool to study fatigue crack propagation in aluminium plates repaired with a composite patch", *Engng. Fract. Mech.*, **99**, 62-78.
- Mhamdia, R., Bachir Bouadjra, B., Serier, B., Ouddad, W., Feaugas, X. and Touzain, S. (2011), "Stress intensity factor for repaired crack with bonded composite patch under thermo-mechanical loading", *J. Reinf. Plast. Compos.*, **30**(5), 416-424.
- Murakami, Y. (1985), *Stress Intensity Factors Handbook*, Vol. I and II, Pergamon Press, Oxford, UK.
- Nikishkov, G.P. and Atluri, S.N. (1987), "Calculation of fracture mechanics parameters for an arbitrary three-dimensional crack, by the 'equivalent domain integral' method", *Int. J. Numer. Meth. Engng.*, **24**(9), 801-821.
- Ouinias, D., Bouiadjra, B.B. and Serier, B. (2007a), "The effects of disbonds on the stress intensity factor of aluminium panels repaired using composite materials", *Compos. Struct.*, **78**(2), 278-284.
- Ouinias, D., Bouiadjra, B.B., Serier, B. and Said Bekkouche, M. (2007b), "Comparison of the effectiveness of boron/epoxy and graphite/epoxy patches for repaired cracks emanating from a semicircular notch edge", *Compos. Struct.*, **80**(4), 514-522.
- Ouinias, D., Bachir Bouiadjra, B., Himouri, S. and Benderdouch, N. (2012), "Progressive edge cracked aluminium plate repaired with adhesively bonded composite patch under full width disbond", *Compos.: Part B*, **43**(2), 805-811.
- Ramji, M. and Srilakshmi, R. (2009), "Design of composite patch reinforcement applied to mixed-mode cracked panel using finite element analysis", *J. Reinf. Plast. Compos.*, **31**(9), 585-595.
- Ramji, M., Srilakshmi, R. and Bhanu Prakash, M. (2013), "Towards optimization of patch shape on the performance of bonded composite repair using FEM", *Compos.: Part B*, **45**(1), 710-720.
- Rice, R. (1968), "A path independent integral and the approximate analysis of strain concentration by notches and cracks", *J. Appl. Mech.*, **35**, 379-386.
- Rose, L.R.F. (1981), "An application of the inclusion analogy for bonded reinforcements", *Int. J. Solid. Struct.*, **17**(8), 827-838.
- Shih, C.F., Moran, B. and Nakamura, T. (1986), "Energy release rate along a three-dimensional crack front in a thermally stressed body", *Int. J. Fract.*, **30**(2), 79-102.
- Srilakshmi, R. and Ramji, M. (2012), "Experimental investigation of adhesively bonded patch repair of an inclined center cracked panel using DIC", *J. Reinf. Plast. Compos.*, **33**(12), 1130-1147.
- Srilakshmi, R., Ramji, M. and Chinthapenta, V. (2015), "Fatigue crack growth study of CFRP patch repaired Al 2024-T3 panel having an inclined center crack using FEA and DIC", *Engng. Fract. Mech.*, **134**, 182-201.
- Turaga, V.R.S. and Ripudaman, S. (1999), "Modelling of a patch repair to a thin cracked sheet", *Engng. Fract. Mech.*, **62**(2), 267-289.